J|A|C|S
COMMUNICATIONS

Published on Web 09/25/2004

Controlled Synthesis of Monodisperse Silver Nanocubes in Water

Dabin Yu and Vivian Wing-Wah Yam*

Center for Carbon-Rich Molecular and Nano-Scale Metal-Based Materials Research and Department of Chemistry, The University of Hong Kong, Pokfulam Road, Hong Kong, P. R. China

Received July 3, 2004; E-mail: wwyam@hku.hk

Controlled synthesis of monodisperse inorganic nanoparticles (NPs) in terms of size and shape has been strongly motivated by the requirements to uncover and map their size- and shape-dependent properties and to achieve their practical applications ranging from biosensing to catalysis, optics, and data storage.[1] Among various NPs, silver NPs are of particular interest because of their wide applications resulting from the unusual properties that depend on their shape and size.[2] The face-centered cubic (fcc) structure of silver metal confers its tendency to nucleate and grow into NPs with their surfaces bounded by the lowest-energy {111} facets, with most of the previous methods, in particular the wet chemical synthesis, being mainly confined to those of the preparation of nanowires, rods, or spheres.[3] Nevertheless, a few of its novel nanostructures, such as the reported disks,[4] prisms, and plates,[2a,5] have attracted great attention. Recently, Xia and co-worker synthesized silver nanocubes with edge length of 115 ± 9 and 95 ± 7 nm by reducing silver nitrate in ethylene glycol.[6] Currently, such kinds of cubic nanostructures have attracted considerable interest because of their important applications. For example, there have been reports on silver nanocubes employed to template formation of gold nanoboxes and iron nanocubes used as the building blocks of magnetic superlattices.[6,7]

Herein we report an alternative new approach to monodisperse silver nanocubes with a mean edge length of 55 ± 5 nm in water by a HTAB-modified silver mirror reaction at 120 °C (HTAB = *n*-hexadecyltrimethylammonium bromide). The silver mirror reaction is an "old" chemical route, which was used to generate reflective mirrors on solid supports.[8] Controlled synthesis of silver nanocubes could be accomplished by such an "old" reaction by the introduction of HTAB. The synthetic reactions were as follows.

$$[Ag(NH_3)_2]^+ (aq) + Br^- (aq) \rightleftharpoons AgBr(s) + 2NH_3 (aq) \quad (1)$$

$$[Ag(NH_3)_2]^+ (aq) + RCHO\ (glucose)\ (aq) \rightarrow Ag\ (NPs) + RCOO^- (aq) + NH_4^+ (aq) \quad (2)$$

Upon addition of HTAB into the solution containing $[Ag(NH_3)_2]^+$, the Br^- from HTAB reacted with $[Ag(NH_3)_2]^+$ to form AgBr (eq 1). This is a reversible reaction with an equilibrium constant of ca. 1.63×10^5 at 120 °C; thus Ag(I) mainly existed in the form of AgBr, resulting in the cathodic shift of the reduction potential of $[Ag(NH_3)_2]^+/Ag$.[9] Consequently, unlike the silver mirror reaction that was normally performed at around room temperature,[10] reaction 2 proceeded in a more controllable manner at such a high temperature to form the nanocubes. With the consumption of $[Ag(NH_3)_2]^+$ by reaction 2, the equilibrium reaction 1 shifts to the left until the reactions are completed.

A typical X-ray diffraction (XRD) pattern of the products is shown in Figure 1, and the peaks were assigned to the diffraction of (111), (200), and (400) planes of fcc silver accordingly. The cell parameter calculated from this pattern was 4.083 Å, in agreement with that found in the literature (PCPDF No. 040783). Interestingly, the (200) diffraction peak showed the strongest intensity in the pattern and its intensity was nearly three times that of the commonly observed strongest (111) diffraction peak (the intensity ratio of (200) to (111) peaks was 40:100, PCPDF No. 040783), and other peaks corresponding to (220), (331), and (222) diffraction were not observed. This indicated that the product had the structure with a preferential [100] orientation. The unusual intensity of the (200) diffraction peak is a result of the strong tendency of the Ag NPs to assemble into two-dimensional (2D) arrays on the solid surface with the *c*-axis perpendicular to the substrate upon the evaporation of the water.[11]

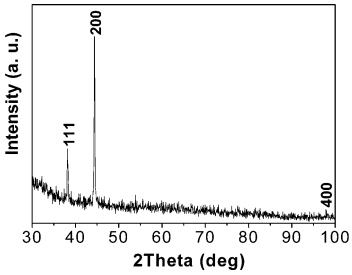

Figure 1. A typical XRD pattern of the Ag nanocubes.

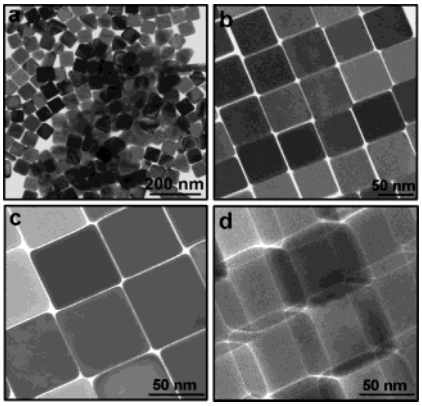

Figure 2. TEM images of Ag nanocubes: (a) with low magnifications; (b−d) with higher magnifications. Images c and d were recorded almost from the same several cubes, but image d was recorded after rotating the cubes by an angle of 30°.

Figure 2a shows a typical transmission electron microscopy (TEM) image of the Ag NPs, indicating that the products consisted of a large quantity of uniform nanocubes. Figure 2b−d shows the TEM images with higher magnifications. Compared to Figure 2c, Figure 2d was recorded after rotating the sample by an angle of 30°, and its remarkable contrast clearly shows a cubic shape of the sample. The TEM analysis indicates that the cubes with smooth faces have a mean edge length of 55 ± 5 nm. The cubes had a strong tendency to assemble into 2D arrays with regular checked pattern on the TEM grid, and the spacings between adjacent cubes

10.1021/ja046037r CCC: $27.50

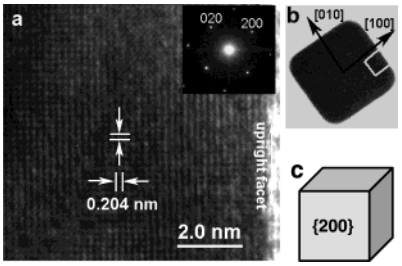

Figure 3. (a) A typical HRTEM image of a selected area of an individual Ag nanocube with the SAED pattern shown in the inset. (b) The nanocube used for the HRTEM and SAED studies with the area marked with a white pane indicating where the HRTEM image was recorded. (c) Schematic illustration of the facets of an individual cube.

are ca. 5 nm. Such a regular assembly of the cubes is due to the facts that the HTAB adsorbed on the cube surfaces would form a capping shell to generate a regular interparticle spacing and thus to prevent the cubes from random aggregation,[12] and that the uniformity of the sample made it possible to manipulate the cubes into a close-packed and ordered array caused by van der Waals forces.[13]

Figure 3a shows the high-resolution TEM (HRTEM) image of a cube as indicated in Figure 3b. The inset shows the corresponding selected area electron diffraction (SAED) pattern, obtained by directing the incident electron beam perpendicular to one of the square facets of the cube. The square spot array was indexed to [200] and [020] of the fcc silver. The 2D lattice fringes of the HRTEM image were examined to be 0.204 nm, close to the {200} lattice spacing of the fcc silver. Because the HRTEM image was recorded from the area along one upright facet as marked by a white pane in Figure 3b, the perpendicular fringes were either parallel to or orthogonal to the upright facet of the cube, suggesting that the six surfaces of the silver nanocubes consisted of {200} lattice planes as schematically illustrated in Figure 3c. Note that our HRTEM images clearly showed that the edges of the cubes were not bounded by {110} as described by Xia,[6] but actually they consisted of small bent faces. On the basis of the TEM and HRTEM analyses, it could be concluded that when these regular nanocubes bounded by {200} facets assembled into a 2D array on a substrate, they, of course, had an identical [001] zone direction, thus resulting in the strongest diffraction of (200) as shown in the XRD pattern.

As an ionic surfactant, HTAB played multiple roles in the formation of the nanocubes. It acted not only as the reaction moderator as described above but also as the shape controller and stabilizing agent. First of all, its micelles directed the silver metal to nucleate and grow into NPs other than the usual silver mirror. As shown in Figure 4a−d, an increase in the molar ratio of HTAB/$[Ag(NH_3)_2]^+$ led to an obvious shape evolution of silver NPs from spheres to cubes, which was caused by the anisotropic adsorption of the surfactant on the silver crystal faces, while such adsorption characteristics depended on the molar ratio.[14] When the molar ratio reached ca. 1.5, anisotropic growth of the particles appeared as indicated by the arrows in Figure 4b. When the molar ratio increased further to 2.5, the product was dominated by nanocubes (Figure 4c). Second, it stabilized the silver NPs to form stable aqueous solutions (Figure 4e), the color of which changed from orange to yellow with the increase of the molar ratio. Note that the nanocubes also showed an absorption band at ca. 420 nm (Figure 4f, curve 4), typical of the plasmon resonance of the spherical silver NPs, since the nanocubes assumed bent edges rather than sharp ones such as triangles or prisms.[2a] More detailed investigation on their optical properties is still in progress.

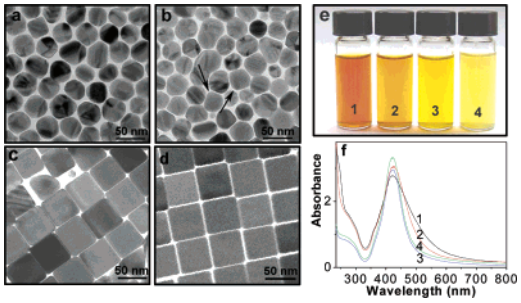

Figure 4. (a−d) TEM images of Ag NPs synthesized with various molar ratios of HTAB/$[Ag(NH_3)_2]^+$: (a) 1, (b) 1.5, (c) 2.5, (d) 3. (e, f) photos and UV/vis absorption spectra of the aqueous solutions of the Ag NPs, marked with 1, 2, 3, and 4 corresponding to those of the Ag NPs shown in panels a, b, c, and d, respectively.

In summary, monodisperse silver nanocubes with edge length of 55 ± 5 nm were, for the first time, synthesized in water on the basis of HTAB-modified silver mirror reaction. Their high stability in water would be favorable for further chemical modification and systematic investigations. Their 2D array with regular checked pattern on solid substrate may open up the possibilities of fabricating new nanodevices with novel physical properties, because the coupling between proximal NPs may give rise to new collective phenomena. Considering the unique properties of silver, its nanocubes should be of importance for both theoretical investigations and practical applications.

Acknowledgment. V.W.-W.Y. acknowledges the financial support from the University Development Fund (UDF) of The University of Hong Kong and The University of Hong Kong Foundation for Educational Development and Research Limited.

Supporting Information Available: Preparation and characterization, calculation of the equilibrium constant, EDX spectrum, HRTEM image and analysis. This material is available free of charge via the Internet at http://pubs.acs.org.

References

(1) (a) Bruchez, M.; Moronne, M.; Gin, P.; Weiss, S.; Alivisatos, A. P. *Science* **1998**, *281*, 2013−2016. (b) Sun, S.; Murray, C. B.; Weller, D.; Folks, L.; Moser, A. *Science* **2000**, *287*, 1989−1992. (c) Wang, J. F.; Gudiksen, M. S.; Duan, X. F.; Cui, Y.; Lieber, C. M. *Science* **2001**, *293*, 1455−1457.
(2) (a) Jin, R.; Cao, Y. C.; Hao, E.; Métraux, G. S.; Schatz, G. Z.; Mirkin, C. A. *Nature* **2003**, *425*, 487−490. (b) Murphy, C. J.; Jana, N. R. *Adv. Mater.* **2002**, *14*, 80−82.
(3) (a) Sun, Y.; Mayers, B.; Herricks, T.; Xia, Y. *Nano Lett.* **2003**, *3*, 955−960. (b) Yin, Y.; Li, Z.; Zhong, Z.; Gates, B.; Xia, Y.; Venkateswaran, S. *J. Mater. Chem.* **2002**, *12*, 522−527.
(4) Hao, E. C.; Kelly, K. L.; Hupp, J. T.; Schatz, G. C. *J. Am Chem. Soc.* **2002**, *124*, 15182−15183.
(5) Sun, Y.; Xia. Y. *Adv. Mater.* **2003**, *15*, 695−699.
(6) Sun, Y.; Xia. Y. *Science* **2002**, *298*, 2176−2179.
(7) Dumestre, F.; Chaudret, B.; Amiens, C.; Renaud, P.; Fejes, P. *Science* **2004**, *303*, 821−823.
(8) Ingalls, A. G. *Amateur Telescope Making (Book One)*; Scientific American Inc.: New York, 1981; p 101.
(9) (a) Rock, P. A. *Chemical Thermodynamics, Principles and Applications*; The Macmillan Company, Collier-Macmillan Ltd: London, 1969; pp 188−190. (b) *Lange's Handbook of Chemistry* (eBook), 15th ed.; Dean, J. A., Ed.; McGraw-Hill: New York, 1999; section 6.
(10) Huang, S.; Mau, A. W. H. *J. Phys. Chem. B* **2003**, *107*, 3455−3458.
(11) *Advances in X-Ray Analysis*; Gilfrich, J. V., Noyan, I. C., Jenkins, R., Huang, T. C., Synder, R. L., Smith, D., Zaitz, M. A., Predecki, P. K., Eds.; Plenum Press: New York and London, 1997; Vol. 39, pp 885−889.
(12) Murray, C. B.; Kagan, C. R.; Bawendi, M. G. *Annu. Rev. Mater. Sci.* **2000**, *30*, 545−610.
(13) Collier, C. P.; Vossmeyer, T.; Heath, J. R. *Annu. Rev. Phys. Chem.* **1998**, *49*, 371−404.
(14) *Handbook of Surface and Colloid Chemistry*, 2nd ed.; Birdi, K. S., Ed.; CRC press: London, 2003; pp 346−385.

JA046037R